Rab18 localizes to lipid droplets and induces their close apposition to the endoplasmic reticulum-derived membrane

Shintaro Ozeki[1,*], Jinglei Cheng[1,*], Kumi Tauchi-Sato[1], Naoya Hatano[2], Hisaaki Taniguchi[2,3] and Toyoshi Fujimoto[1,‡]

[1]Department of Anatomy and Molecular Cell Biology, Graduate School of Medicine, Nagoya University, 65 Tsurumai, Showa, Nagoya 466-8550, Japan
[2]Harima Institute at SPring-8, RIKEN, Mikazuki, Sayo, Hyogo 679-5148, Japan
[3]Institute for Enzyme Research, The University of Tokushima, Tokushima 770-8503, Japan
*These authors contributed equally to this work
‡Author for correspondence (e-mail: tfujimot@med.nagoya-u.ac.jp)

Accepted 17 March 2005
Journal of Cell Science 118, 2601-2611 Published by The Company of Biologists 2005
doi:10.1242/jcs.02401

Summary

Lipid droplets (LDs) are organelles that store neutral lipids, but their regulatory mechanism is not well understood. In the present study, we identified Rab18 as an LD component of HepG2 cells by proteomic analysis, and confirmed its localization by immunohistochemistry and western blotting. Wild-type and dominant-active Rab18 localized to LDs but the dominant-negative form did not. Endogenous Rab18 coexisted with adipocyte differentiation-related protein (ADRP) in LDs, but the labeling intensity of the two proteins showed clear reciprocity. Consistent with this observation, overexpression of Rab18 induced a decrease in the amounts of ADRP in LDs in HepG2 and BALB/c 3T3 cells. Furthermore, Rab18 overexpression caused close apposition of LDs to membrane cisternae connected to the rough ER. Two other procedures that decrease ADRP, i.e. RNA interference and brefeldin A treatment, induced the same morphological change, indicating that decrease in ADRP was the cause of the LD-ER apposition. In accordance with similar structures found between ER and other organelles, we propose that the ER membrane apposed to LDs should be named the LD-associated membrane, or LAM. The present results suggested that Rab18 regulates LAM formation, which is likely to be involved in mobilizing lipid esters stored in LDs.

Key words: Lipid droplet, Mass spectrometry, Rab18, Endoplasmic reticulum, Membrane apposition

Introduction

Lipid droplets (LDs) are found in many kinds of cells. Their surface is composed of a phospholipid monolayer containing free cholesterol, and the core is a mixture of lipid esters, mostly triglyceride and cholesterol ester (Murphy and Vance, 1999; Tauchi-Sato et al., 2002). In adipocytes, LDs store triglyceride, which is used as the source of energy production; in steroid-producing cells, cholesterol ester is stored in LDs for the synthesis of steroid hormones. However, the physiological function of LDs in other cell types has attracted little attention until recently, and LDs were generally thought to be inert and static organelles for storage of excess lipid.

LDs in non-adipose cells have been shown to harbor adipocyte differentiation-related protein (ADRP) and TIP47, both of which show sequence similarity to perilipin expressed in adipose cells (Londos et al., 1999). However, studies performed over the past several years have revealed that LDs contain a number of other functional molecules including major eicosanoid-forming enzymes (Bozza et al., 1997), MAP kinase, cytosolic phospholipase A2 (Yu et al., 1998), caveolins (Fujimoto et al., 2001; Ostermeyer et al., 2001; Pol et al., 2001), α-synuclein (Cole et al., 2002), Nir2 (Litvak et al., 2002), NAD(P)H steroid dehydrogenase (Ohashi et al., 2003), and σ-1 receptor (Hayashi and Su, 2003). In conjunction with the mobility and rapid transport of various lipids in and out of LDs (Frolov et al., 2000; Prattes et al., 2000; Pol et al., 2004), it is becoming clear that LDs are much more dynamic and functionally active organelles than originally thought.

To elucidate the physiological functions of LDs in molecular terms, we attempted to identify molecules involved in LD function by a proteomic approach. After our preliminary report (T.F., Noriko Nakamura, S.O. and Hiroshi Kogo, The 75th Annual Meeting of the Japanese Biochemical Society, Kyoto, Japan, 2002), three groups published the results of proteomic studies of LDs from various cell types (Fujimoto et al., 2004; Liu et al., 2004; Umlauf et al., 2004). One of a number of proteins identified by the proteomic analysis is Rab18, which we have investigated and found to be highly concentrated in LDs, and that its expression reduced ADRP from LDs. Furthermore, Rab18 induced close apposition of LDs to an ER-derived membrane. These observations implied that Rab18 plays a crucial role in controlling the relationship between LDs and the ER, which may be important for lipid transport between the two organelles.

Materials and Methods

Cells and antibodies

Human HepG2 and mouse BALB/c 3T3 cells were obtained from the Japanese Collection of Research Bioresources Cell Bank. The cells were maintained in Dulbecco's minimum essential medium supplemented with 10% fetal calf serum (FCS), 50 U/ml penicillin and 0.05 mg/ml streptomycin at 37°C under 5% CO_2/95% air.

Anti-Rab18 antibody was raised in rabbits by injecting an antigen peptide (ESENQNKGVKLSH), corresponding to amino acids 177-189 of human Rab18, bound to keyhole limpet hemocyanin, and affinity-purified by an antigen column. We verified that the antibody does not react with Rab1, Rab2, Rab3, Rab5, Rab7, Rab9 or Rab10 by immunofluorescence microscopy and western blotting using cells transfected with the respective Rab cDNA. Antibodies to lysobisphosphatidic acid (LBPA) (Kobayashi et al., 1998), and LC3 (Kabeya et al., 2000) were kindly provided by Toshihide Kobayashi and Yasuo Uchiyama, respectively. Antibodies: ADRP (Progen, Darra, Australia), Lamp1 and Myc (Developmental Studies Hybridoma Bank, the University of Iowa, USA), EEA1 (Transduction Lab., Lexington, KY, USA), transferrin receptor (Cymbus Biotech., Flanders, NJ, USA), GFP (Molecular Probes, Eugene, OR, USA), and FLAG (Sigma-Aldrich, St Louis, MO, USA). Secondary antibodies conjugated with fluorochromes (Molecular Probes) and colloidal gold (BioCell, Cardiff, UK) were also used.

Expression vectors and siRNA

cDNAs of human Rab1, Rab9 and Rab18 were amplified from HepG2 or human fibroblast total RNA by RT-PCR, checked by sequencing and cloned in pEGFP-C (Clontech, Palo Alto, CA, USA) and pFLAG-C (Sigma-Aldrich) vectors. pEFBOS-Myc-Rab2, pCMV5-FLAG-Rab5, pEGFP-Rab7 and pEGFP-Rab10 were kindly provided by Yoshimi Takai, Toshiaki Katada, Takuya Sasaki and Mitsunori Fukuda, respectively. Small interfering RNA (siRNA) for ADRP knockdown was produced by either in vitro transcription using an siRNA construction kit (Ambion, Austin, TX, USA) or by chemical synthesis by Japan BioService (Saitama, Japan). Both plasmid expression vectors and siRNAs were transfected into cells by Lipofectamine2000 (Invitrogen, San Diego, CA, USA) according to the manufacturer's instruction. Cells were used 24-48 hours after transfection of plasmid vectors, and 48-72 hours after siRNA treatment.

Isolation of LDs by subcellular fractionation

LDs were isolated from HepG2 cells as described (Fujimoto et al., 2001). Briefly, cells were disrupted by nitrogen cavitation at 800 psi for 15 minutes at 4°C. After the nuclei were sedimented, the supernatant, adjusted to 0.54 M sucrose (3 ml), was overlaid with 0.27 M sucrose (3 ml), 0.135 M sucrose (3 ml) in disruption buffer, and buffer without sucrose (3 ml), followed by centrifugation for 60 minutes at 154,000 ***g*** in an SW41 rotor (Beckman, Fullerton, CA, USA). The LD fraction recovered at the top of the tube was used for mass analysis. For western blotting, eight fractions (1.5 ml each) were obtained from the top, mixed with 6× sample buffer, and subjected to electrophoresis and electrotransfer.

Proteomic analysis

The LD fraction purified from HepG2 cells was subjected to proteomic analysis as described previously (Kikuchi et al., 2004). Briefly, the sample electrophoresed in SDS-PAGE was stained with Coomassie Brilliant Blue, destained, and subjected to in-gel digestion with trypsin after reduction by dithiothreitol and alkylation by iodoacetamide. The resulting peptides were extracted and subjected to liquid chromatography/mass spectrometry (LC/MS) and data-dependent tandem mass (LC-MS/MS) analyses using a Q-Tof-type hybrid mass spectrometer (Micromass, Manchester, UK) interfaced on-line with a capillary HPLC (Waters-Micromass modular CapLC, Micromass). Peak lists obtained from the MS/MS spectra were used to identify proteins using the Mascot search engine (Matrixscience, London, UK).

Immunofluorescence microscopy

Cells cultured on coverslips were observed by immunofluorescence microscopy as described previously (Fujimoto et al., 2001). For most experiments, cells were fixed with 3% formaldehyde and 0.05-0.1% glutaraldehyde, permeabilized with 0.01% digitonin, and treated with 3% bovine serum albumin (BSA) before immunolabeling. LDs were visualized using BODIPY493/503 (Molecular Probes) in most experiments (Gocze and Freeman, 1994). When triple labeling was necessary, LDs were stained with Sudan III. Although the procedure for Sudan III staining could cause some morphological changes in the LDs, correlations with antigen localization were preserved (Fukumoto and Fujimoto, 2002). Images were acquired using a Zeiss PASCAL confocal laser scanning microscope, or a Zeiss Axiophot2 fluorescence microscope equipped with an AxioCam digital camera.

Conventional and immunoelectron microscopy

For conventional electron microscopy, cells on coverslips were fixed with 2.5% glutaraldehyde, post-fixed with 1% osmium tetroxide, stained en bloc with uranyl acetate, and embedded in Epon for thin sectioning. For some specimens, 0.7% potassium ferrocyanide was added to the osmium tetroxide solution to enhance membrane contrast. For immunoelectron microscopy, cells were fixed with 3% formaldehyde for 60 minutes, infiltrated with a mixture of sucrose and polyvinylpyrolidone, and frozen in liquid nitrogen. Ultrathin cryosections were prepared, labeled with antibodies, and embedded in methylcellulose (Liou et al., 1996). The specimens were observed using a JEOL 1200CX electron microscope operated at 100 kV.

Results

Identification of Rab18 as an LD constituent

LDs were purified from HepG2 cells, and their purity was verified by western blotting as described in the following section. Proteins were electrophoresed, cut into slices, subjected to in-gel digestion, and the resulting peptide mixtures were analyzed by LC-MS/MS (Kikuchi et al., 2004). Besides adipocyte differentiation-related protein (ADRP) and TIP47 (Londos et al., 1999; Miura et al., 2002), which have been shown to be LD components, more than 50 proteins were identified using the Mascot search engine. The overall profile was similar to the result reported recently by two other groups (Liu et al., 2004; Umlauf et al., 2004). The results regarding some of these proteins will be discussed in separate papers.

A number of Rab proteins were identified by proteomic analysis, i.e. Rab1, Rab2, Rab5, Rab6, Rab7, Rab8, Rab10, Rab11, Rab14, Rab18 and Rab32. To examine the extent to which the Rab proteins exist in LDs, we transfected cells with tagged Rab cDNAs and observed their distribution in comparison with LDs stained with BODIPY493/503 or Sudan III. Six Rabs, Rab1, Rab2, Rab5, Rab7, Rab10 and Rab18, were examined. Among these Rab proteins, only Rab18 showed conspicuous and almost exclusive labeling around LDs, whereas other Rabs were generally distributed in other parts of the cell or were distributed rather diffusely in the cytoplasm, and only a small number were seen around LDs (Fig. 1A). The LD localization of Rab18 was seen when either

FLAG or EGFP was used as a tag, and even when EGFP-Rab18 was observed without permeabilization. These results excluded the possibility of artifacts caused by the tag or the labeling procedure.

To compare the LD localization of the Rabs objectively, quantification was performed by two methods. First, the proportion of the LDs stained with BODIPY493/503 that were Rab-positive was determined. Only those LDs encircled completely by Rab labeling were counted as positive, and those seen adjacent to these Rabs or only partially surrounded by labeling were not included (Fig. 1B). Second, the proportion of cells in which more than 10% of the LDs were Rab-positive was determined (Fig. 1C). By either method, a high percentage of Rab18 was found to be localized to LDs. The other Rabs were also found around LDs, but only in much lower ratios than Rab18. Despite their less frequent LD localization, the functions of these Rabs may be related to LDs in some way. However, in the present study, we concentrated on Rab18 because of its conspicuous localization to LDs.

We next examined whether the LD localization of Rab18 was dependent on its activation. Based on the highly conserved sequence among Rab proteins, we constructed a GTPase-deficient mutant (Q67L) and a constitutively GDP-bound mutant (S22N) of Rab18, and observed the distribution of EGFP- and FLAG-tagged molecules in HepG2 cells. Rab18(Q67L) showed localization to LDs in the same way as Rab18(WT: wild-type), whereas Rab18(S22N) was seen diffusely in the cytoplasm and did not show any concentration around LDs (Fig. 1D). These observations implied that the localization of Rab18 to LDs

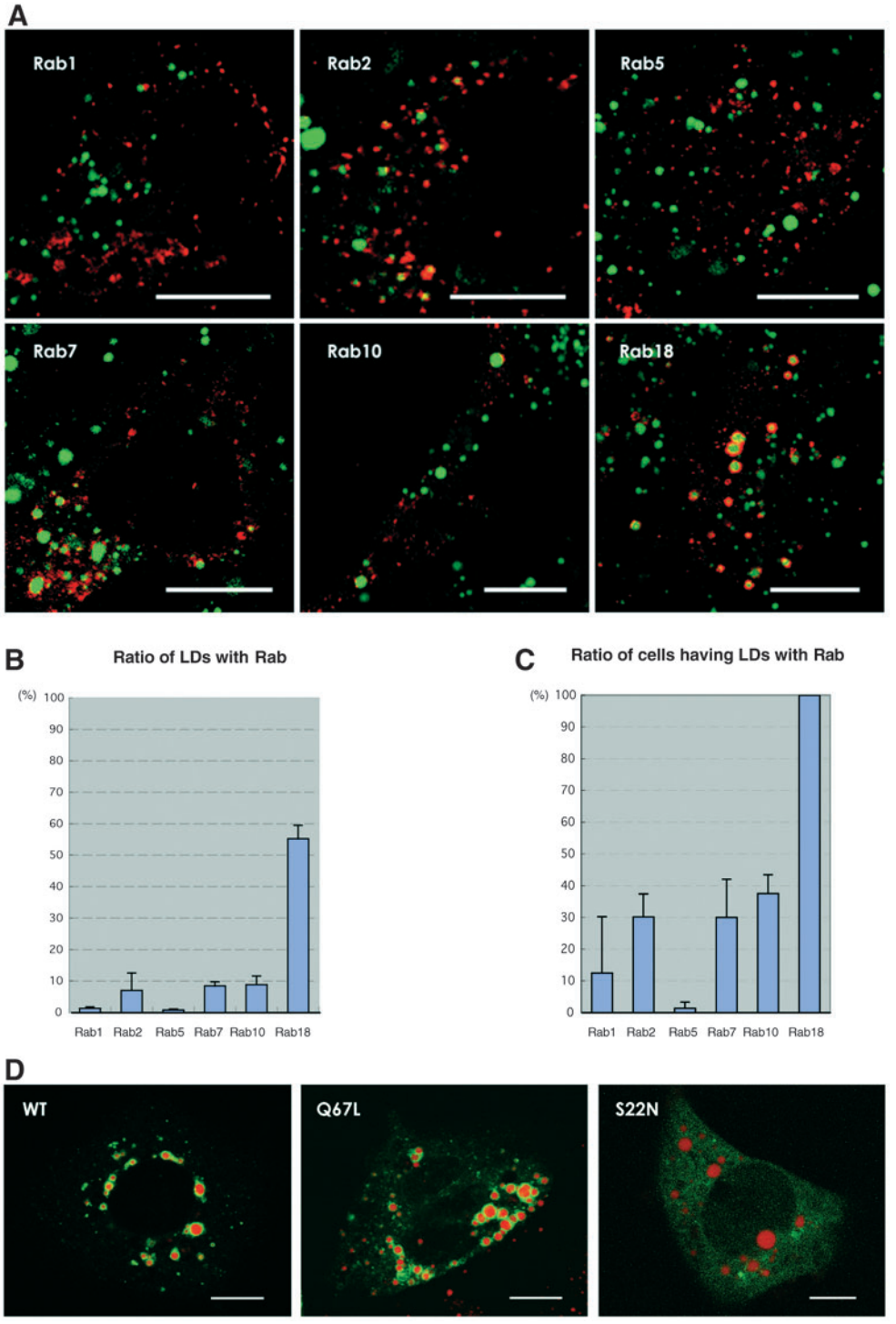

Fig. 1. (A) Double labeling of Rab proteins (red) and LDs (green) in HepG2 cells. Cells were transfected with cDNA of tagged Rab proteins. LDs were stained with BODIPY 493/503. Rab1, Rab5, Rab7, Rab10 and Rab18 were tagged with FLAG, and Rab2 was tagged with Myc. Rab18 was consistently concentrated around LDs, whereas other Rabs were observed in the vicinity of LDs only infrequently. Bars, 10 μm. (B) The proportion of Rab-positive LDs among all the LDs stained with BODIPY 493/503. Only cells showing positive Rab labeling were selected and counted. More than 500 LDs in 10 random areas were counted in two independent experiments. (C) The proportion of cells in which the Rab-positive LDs were more than 10% of the total detected LDs. Only cells showing positive Rab labeling were selected and counted. More than 30 cells in 10 random areas were counted in two independent experiments. (D) Double labeling of EGFP-tagged Rab18 (green) and LDs (red) in HepG2 cells. The distributions of wild-type Rab18(WT) and GTPase-deficient Rab18(Q67L) were confined to LDs stained with Sudan III, while constitutively GDP-bound Rab18(S22N) was observed diffusely in the cytoplasm. Scale bars: 10 μm.

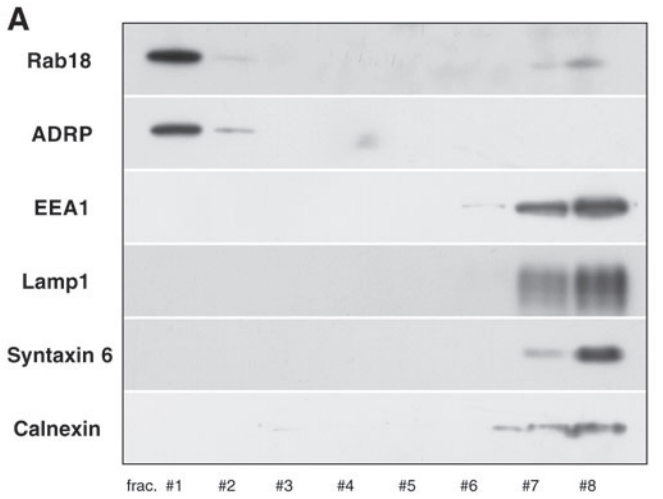

Fig. 2. (A) Western blotting of sucrose density-gradient fractions from HepG2. An equal volume from each fraction was loaded. Both ADRP and Rab18 were strongly present in the top floating LD fraction (#1). There was also some Rab18 in the bottom fractions containing soluble and membrane proteins (#7, #8). EEA1, Lamp1, syntaxin 6,and calnexin were detected only in the bottom fractions (#6-8). (B) Double labeling of endogenous Rab18 (red) and LDs (green) in HepG2 cells. LDs were stained with BODIPY 493/503. Antibody labeling for Rab18 was concentrated around LDs. Note that there were LDs that were not associated with anti-Rab18 (arrowheads). Scale bar: 10 μm. (C) Double labeling of endogenous Rab18 (green) and endosomal markers (red). EEA1 and transferrin receptor (Tf-R) (upper panel), and lysobisphosphatidic acid (LBPA) and Lamp1 (lower panel) were used as markers for early and late endosomes, respectively. Rab18 did not show co-distribution with any of the endosomal markers. Scale bars: 10 μm.

is regulated by its guanine nucleotide status.

Localization of endogenous Rab18

We raised a polyclonal anti-Rab18 antibody in rabbits using a synthetic peptide as the antigen. On western blotting, the antibody reacted specifically with a 23 kDa band from human and mouse samples. Cross-reactivity with other Rabs was checked by applying the antibody to cell samples transfected with tagged Rab proteins (i.e. Rab1, Rab2, Rab3, Rab5, Rab7, Rab9 and Rab10); in both immunofluorescence microscopy and western blotting, the antibody was confirmed not to react with the other Rabs (data not shown).

Western blotting of subcellular fractions of HepG2 showed that the anti-Rab18 antibody reacted intensely with the top floating fractions, which were highly enriched with LDs, as shown by its reactivity with anti-ADRP (Fig. 2A). When gels were loaded with an equal volume from each fraction, the immunoreactivity for Rab18 was also seen in the bottom fractions containing membrane and soluble proteins. The purity of the LD fraction was confirmed by the absence of other organelle markers; EEA1 for the early endosome, Lamp1 for the late endosome/lysosome, syntaxin 6 for the *trans*-Golgi network, and calnexin for the ER were only detected in the bottom fractions. In our previous study we also showed that markers for the Golgi apparatus, ER and the plasma membrane were not found in the LD fraction (Fujimoto et al., 2001).

Using immunofluorescence microscopy of HepG2 and 3T3 cells, the anti-Rab18 antibody was shown to be present in a ring around BODIPY493/503-stained LDs (Fig. 2B). Notably, a subpopulation of LDs were not labeled by anti-Rab18 antibody (arrowheads in Fig. 2B). The labeling was abolished by pre-absorption of the anti-Rab18 antibody with the antigen peptide or when it was omitted from the procedure (data not shown). These observations supported the results of LC-MS/MS and immunofluorescence microscopy of tagged Rab18, and demonstrated that endogenous Rab18 was localized to LDs.

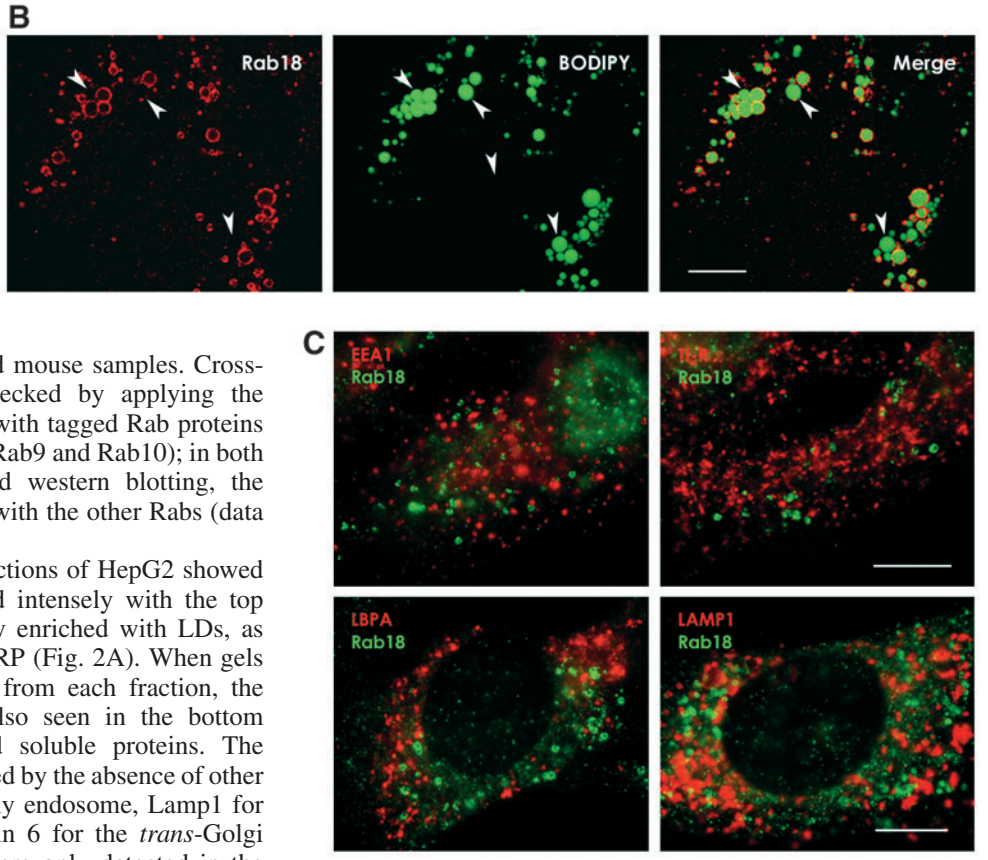

A previous study showed that Rab18 was distributed in the endosomal vesicles of MDCK cells (Lutcke et al., 1994). To examine this possibility, double labeling for Rab18 and endosomal markers was performed. For the late endosome, we labeled for LBPA and Lamp1, and for the early endosome, we labeled for EEA1 and transferrin receptor. However, Rab18 did not overlap with any of the endosomal markers (Fig. 2C). Based on the result of immunofluorescence microscopy and western blotting, we concluded that Rab18 was localized to the LDs in the cell types examined. The disparity between the present result and those reported previously (Lutcke et al., 1994) cannot be explained easily, but it is notable that a similar disparity with regard to the localization of TIP47 has been

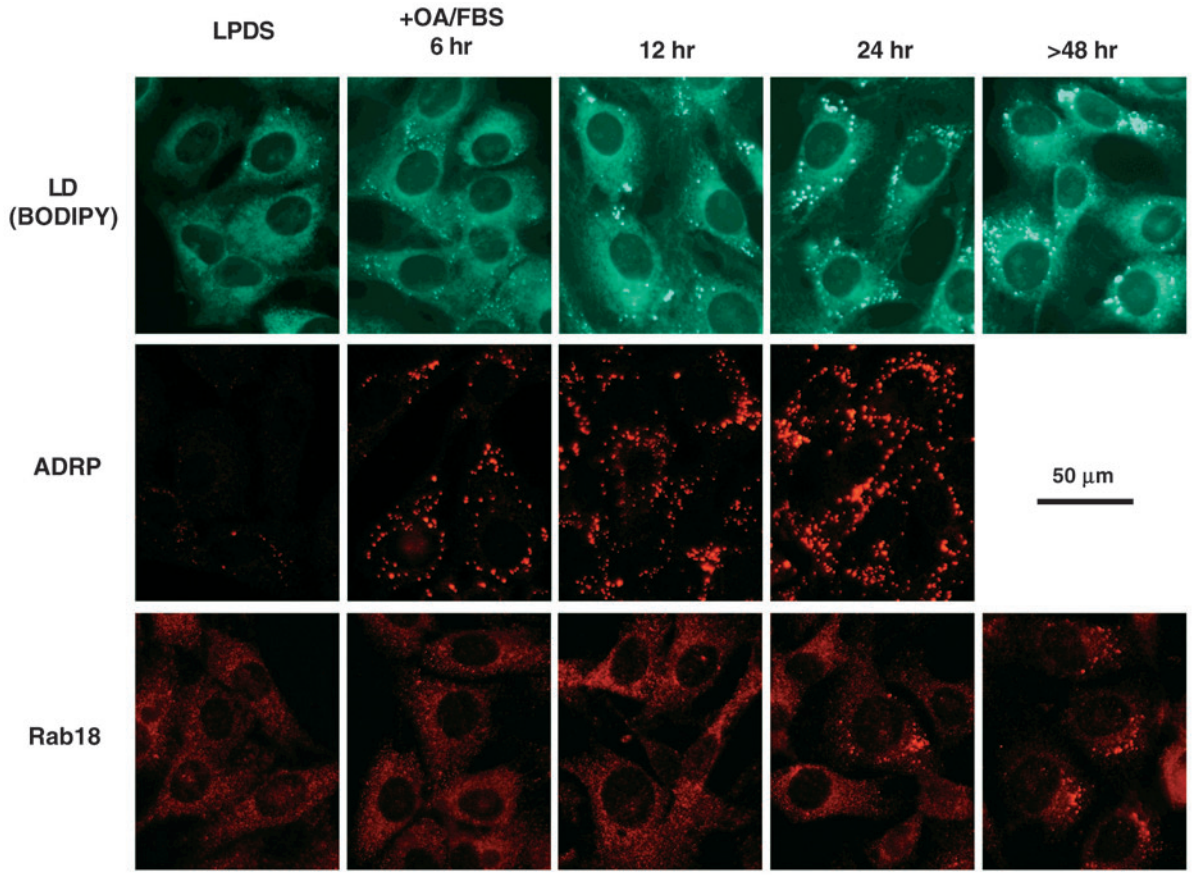

Fig. 3. Time course of LD formation (stained with BODIPY 493/503) in relation to ADRP and Rab18 in 3T3 cells loaded with oleic acid. Cells were cultured in medium containing 2% LPDS for 2 days, and then transferred to medium with 10% FBS with 200 μM oleic acid-BSA complex (OA/FBS). LDs, ADRP and Rab18 were not detected in the cells kept in LPDS. As early as 6 hours after transfer to OA/FBS medium, LDs and ADRP were observed as bright dots that increased in number and brightness thereafter. In contrast, Rab18 was barely visible as dots at 6 or 12 hours in OA/FBS medium, and was seen clearly only after 24 hours in OA/FBS medium.

reported by other groups (Barbero et al., 2001; Wolins et al., 2001; Miura et al., 2002). Proteins that have a propensity to localize to LDs may be affected by subtle differences in experimental conditions, and may be distributed in other locations under some circumstances.

To examine the time course of ADRP and Rab18 appearance in relation to de novo LD formation, 3T3 cells were cultured in the presence of 2% lipoprotein-deficient serum (LPDS) for 2 days, followed by the addition of 200 μM oleic acid (OA) complexed to BSA in 10% FCS. Before the addition of OA and FCS, none of the labels were detected as fluorescent dots (Fig. 3). Six hours after the addition of OA and FCS, LDs appeared, and ADRP was observed as ring-shaped fluorescence around them. In contrast, Rab18 fluorescence was very weak at 6 hours; although it became detectable at later time points, the frequency of labeling was far less than that of ADRP.

Effect of Rab18 overexpression on LDs

When triple labeling of endogenous Rab18, ADRP and LDs was performed in HepG2, both Rab18 and ADRP were shown to be associated with BODIPY 493/503-positive LDs as expected. However, the labeling intensity of Rab18 and ADRP showed clear reciprocity in most cases, i.e. in LDs where the Rab18 labeling was intense, ADRP labeling was relatively weak, and vice versa (Fig. 4A). These results suggested that the presence of Rab18 may decrease the amount of ADRP in LDs. Therefore, we examined the consequences of Rab18 overexpression on ADRP. When EGFP-Rab18(WT) was introduced, it was distributed around Sudan III-positive LDs in HepG2 cells, but EGFP-Rab18(WT) and ADRP hardly overlapped (Fig. 4B). The reduction of ADRP expression in the Rab18-overexpressing cell was also detected by western blotting of the total cell lysate. The cells transfected with non-tagged Rab18 cDNA expressed lower levels of ADRP than those transfected with empty vector (Fig. 4C). Similar results were obtained when cells transfected with EGFP-Rab18 cDNA were compared with those transfected with EGFP cDNA (data not shown).

The reduction of ADRP in LDs expressing Rab18 was further confirmed by triple labeling (Fig. 4D): BODIPY 493/503-positive LDs harboring EGFP-Rab18(WT) lacked or showed little ADRP labeling, and those with intense ADRP labeling were devoid of EGFP-Rab18(WT). The exclusion of ADRP from LDs was also observed when FLAG-tagged Rab18(WT) was introduced, verifying that the EGFP tag was not the cause of the phenomenon (data not shown). EGFP-Rab18(Q67L) gave the same result, but neither EGFP alone nor EGFP-Rab18(S22N) affected the labeling of ADRP in LDs

(Fig. 4D). Reciprocity of EGFP-Rab18 and ADRP was also seen when isolated LDs were labeled with anti-ADRP and observed in comparison with EGFP-Rab18 (Fig. 4E). These results indicated that overexpression of Rab18 reduces the amount of ADRP in LDs.

Ultrastructural analysis of Rab18-overexpressing cells

To confirm that EGFP-Rab18 was localized to the LD surface, ultrathin cryosections of transfected cells were prepared and labeled with anti-GFP. Immunogold labeling was indeed seen along the surface of LDs, although LDs were usually observed

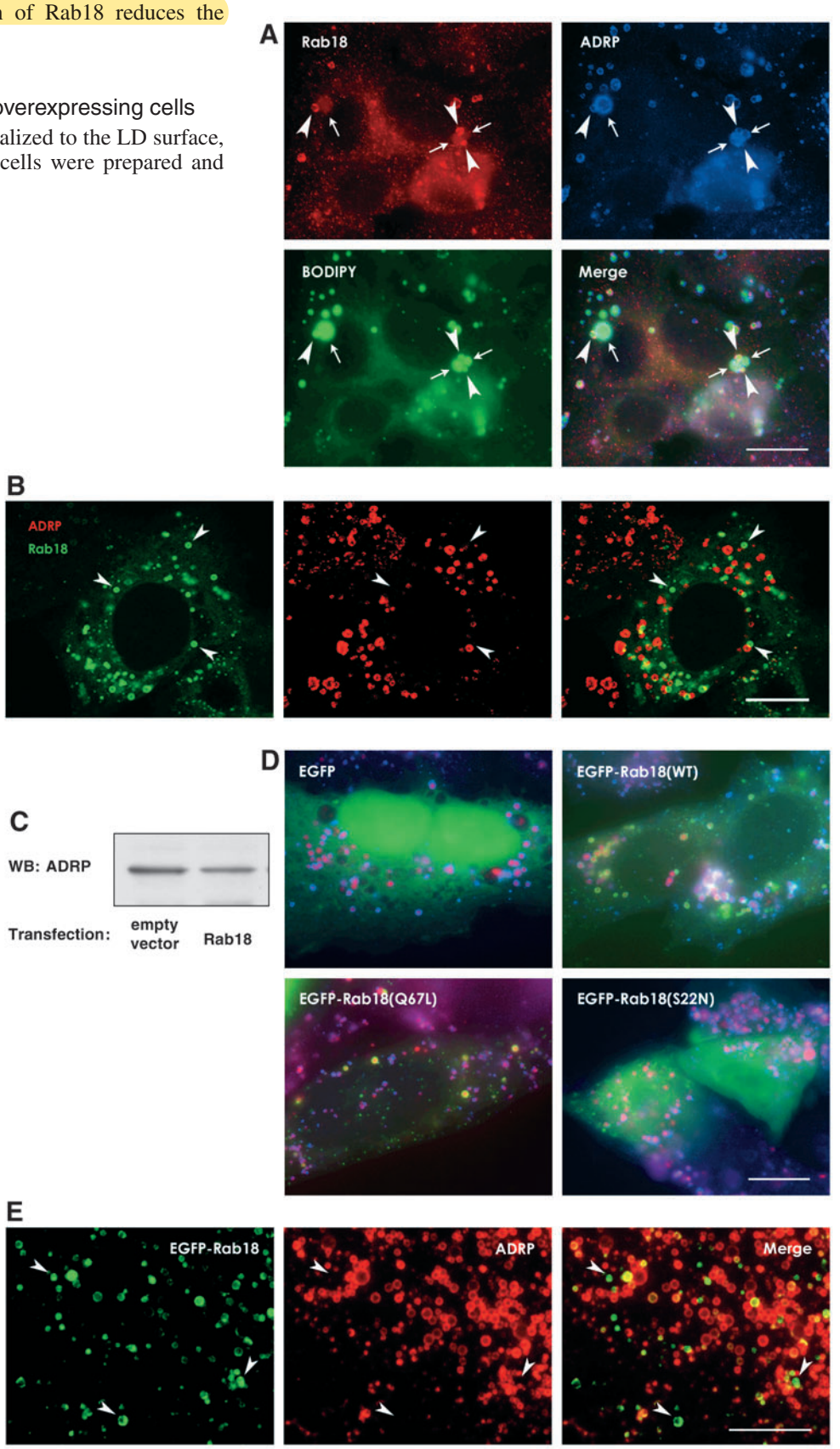

Fig. 4. (A). HepG2 cells were triple labeled for endogenous Rab18 (red), ADRP (blue), and LDs (green). BODIPY 493/503-stained LDs were labeled for Rab18 and ADRP, but the labeling intensity for Rab18 and ADRP appeared to be reciprocal in most cases. LDs showing strong Rab18 and weak ADRP staining are indicated by arrowheads, and those with the reverse pattern are indicated by arrows. Scale bar: 10 μm. (B) HepG2 cells transfected with EGFP-Rab18(WT) cDNA were labeled with anti-ADRP. Both EGFP-Rab18(WT) (green) and ADRP (red) are visible as small rings of fluorescence, but there is very little overlap. Some Rab18-positive, ADRP-negative ring-shaped fluorescent signals are marked by arrowheads. Scale bar: 10 μm. (C) Western blotting of ADRP. HepG2 cells were transfected with empty vector or Rab18 cDNA. Equal amounts (20 μg) of the total cell lysates were electrophoresed and probed with anti-ADRP antibody. Expression of Rab18 caused a reduction of ADRP. (D) 3T3 cells, expressing EGFP, EGFP-Rab18(WT), EGFP-Rab18(Q67L), or EGFP-Rab18(S22N) (green), were further labeled with anti-ADRP (blue) and Sudan III (red). Merged images of the three colors are shown. EGFP and EGFP-Rab18(S22N) were distributed diffusely in the cytoplasm, and all the Sudan III-positive LDs were labeled with anti-ADRP. In contrast, in cells expressing EGFP-Rab18(WT) or EGFP-Rab18(Q67L), LDs were labeled for either EGFP-Rab18 or ADRP, and those showing both labels were scarce. Scale bar: 10 μm. (E) LDs isolated from HepG2-expressing EGFP-Rab18(WT) (green) were labeled with anti-ADRP (red). LDs with strong EGFP-Rab18(WT) fluorescence generally showed weak ADRP labeling. EGFP-Rab18(WT)-positive, ADRP-negative LDs are indicated by arrowheads. Scale bar: 10 μm.

as an empty round space because of the difficulty of retaining lipid ester in ultrathin cryosections (Fig. 5A). At the same time, we often noticed thin membrane cisternae in the vicinity of EGFP-Rab18-positive LDs (arrows in Fig. 5A).

To clearly delineate the membrane cisterna, we examined resin-embedded sections of 3T3 cells transfected with EGFP-Rab18(WT). As observed in ultrathin cryosections, the cell frequently showed LDs apposed closely to thin membrane cisternae; occasionally LDs were encircled completely by the cisterna (Fig. 5B). The cisterna was often found to be continuous with the rough endoplasmic reticulum (ER) or was studded with ribosomes. In contrast, such extensive membrane apposition to LDs was seen only rarely in cells transfected with EGFP cDNA or in untreated control cells (Fig. 5C). The frequency of cells with LDs apposed to the membrane cisterna was counted in electron micrographs (Fig. 5F); more than 30 cells were taken at random, and LDs with closely apposed membranes over more than half of the perimeter were defined as positive. The frequencies were 41.4% in cells transfected with EGFP-Rab18(WT) cDNA and 3.4% in cells transfected with EGFP cDNA. In the present study, cells were used after transient transfection because more than 60% of the cells were transfected as judged by fluorescence microscopy. Several stably transfected cell lines were also prepared, but even after subcloning only 20-50% of the cells showed fluorescence. They showed LD-membrane apposition, but the frequency was lower than that of the transiently transfected cells.

The ER-derived membrane apposed to LDs was not likely to be the autophagic vacuole, because LC3, a marker of early autophagic vacuoles (Kabeya et al., 2000), was not detected around the EGFP-Rab18-positive LDs by immunofluorescence microscopy, and autophagic vacuoles did not appear to be increased in cells expressing EGFP-Rab18 as determined by electron microscopy (data not shown).

Down-regulation of ADRP induces membrane apposition to LDs

The above results demonstrated that overexpression of Rab18 causes a decrease in the level of ADRP in LDs as well as close membrane apposition between LDs and the ER-derived membrane. To examine whether the decrease in ADRP in LDs was the cause of the membrane apposition, we applied two different methods to decrease ADRP and examined whether similar structural changes were induced: one was knockdown of ADRP by RNA interference, and the other was brefeldin A (BFA) treatment.

For RNA interference, cells transfected with siRNA for ADRP knockdown were compared with those transfected with control scrambled siRNA. About 50% reduction of ADRP expression was verified by western blotting (Fig. 5D-1). By electron microscopy, cells treated with ADRP siRNA frequently showed LDs surrounded by the neighboring membrane cisternae (48.1%), which were very similar to the structure in Rab18-overexpressing cells. In contrast, such structures were hardly observed in cells treated with control siRNA (3.7%) (Fig. 5D-2,F).

In a previous study, we observed that the amount of ADRP in LDs was reduced significantly by treating cells with BFA (Nakamura et al., 2004). Electron microscopy of cells treated with BFA for 5 hours showed that LDs were surrounded by thin membrane cisternae in the majority of cells (82.8%). Such a disposition was seldom observed in control untreated cells (6.9%; Fig. 5E,F). Virtually all LDs in BFA-treated cells showed apposition to the ER, whereas in cells transfected with pEGFP-Rab18 cDNA or ADRP siRNA, LDs showing apposition to the ER coexisted with those without such a disposition. This difference can be explained at least partly by the penetration ratio of the procedures: BFA should affect all the cells and LDs with the same strength, but the ratio of transfected cells was about 60-70% with variable intensity as estimated by fluorescence microscopy.

Discussion

Rab proteins in LDs

By proteomic analysis of purified LDs, we found that a number of Rab proteins exist in LDs, observations that were similar to the reports by two other groups (Liu et al., 2004; Umlauf et al., 2004). Tagged Rabs were distributed around LDs to variable degrees, but with the exception of Rab18, they were mostly distributed to locations other than the LDs, and only a fraction of the labeling was found around LDs. The relative scarcity of these Rabs in LDs does not necessarily exclude their functional significance, and they might be further recruited to LDs under some circumstances. However, owing to the unique characteristics of the LD surface (Tauchi-Sato et al., 2002), it is possible that some of the Rabs adhered to the LDs during the purification procedure. Further studies are required to determine whether the existence of a variety of Rabs in the purified LD samples has any physiological significance.

Mechanism by which Rab18 causes elimination of ADRP from LD

When cells were transfected with Rab18 cDNA, LDs harboring exogenous Rab18 showed weaker ADRP labeling than the others. This observation can be explained if expression of Rab18 induces de novo formation of LDs containing little ADRP, but the following results indicated that Rab18 was recruited to pre-existing LDs and replaced ADRP. First, overexpression of Rab18 did not increase the number or the total volume of LDs observed by fluorescence microscopy (data not shown); second, even when HepG2 cells were cultured in 2% LPDS to minimize de novo LD formation, recruitment of Rab18 to remaining LDs occurred to a similar extent.

These observations raise the question of how Rab18 decreases ADRP in LDs. Interestingly, ADRP is also eliminated from LDs by expression of perilipin (Brasaemle et al., 1997) and hepatitis C virus (HCV) core protein (data cited in McLauchlan, 2000). We also observed that the N-terminal truncation mutant of caveolin-3 that is distributed to LDs (Pol et al., 2001) also displaced ADRP (K.T.-S. and T.F., unpublished). However, it is unlikely that these proteins compete with ADRP for common specific binding sites in LDs for several reasons. First, in the case of perilipin, despite some similarity to ADRP in the N-terminal PAT-1 domain (Londos et al., 1999), binding to LDs is not mediated by the domain, but by the adjacent short hydrophobic segments (Garcia et al., 2003; Garcia et al., 2004). Second, targeting of HCV core protein and caveolins to LDs requires a long

hydrophobic domain (Hope and McLauchlan, 2000; Fujimoto et al., 2001; Ostermeyer et al., 2004), which is not found in ADRP or perilipin. Third, Rab18 does not appear to have any structural similarity to ADRP, perilipin, or HCV core protein. These properties suggest that any proteins recruited to the LDs in large amounts could replace pre-existing ADRP sterically. Alternatively, the above proteins could recruit a common protein(s), which competes with ADRP in adherence to LDs. In the case of Rab18, effector proteins may also be involved.

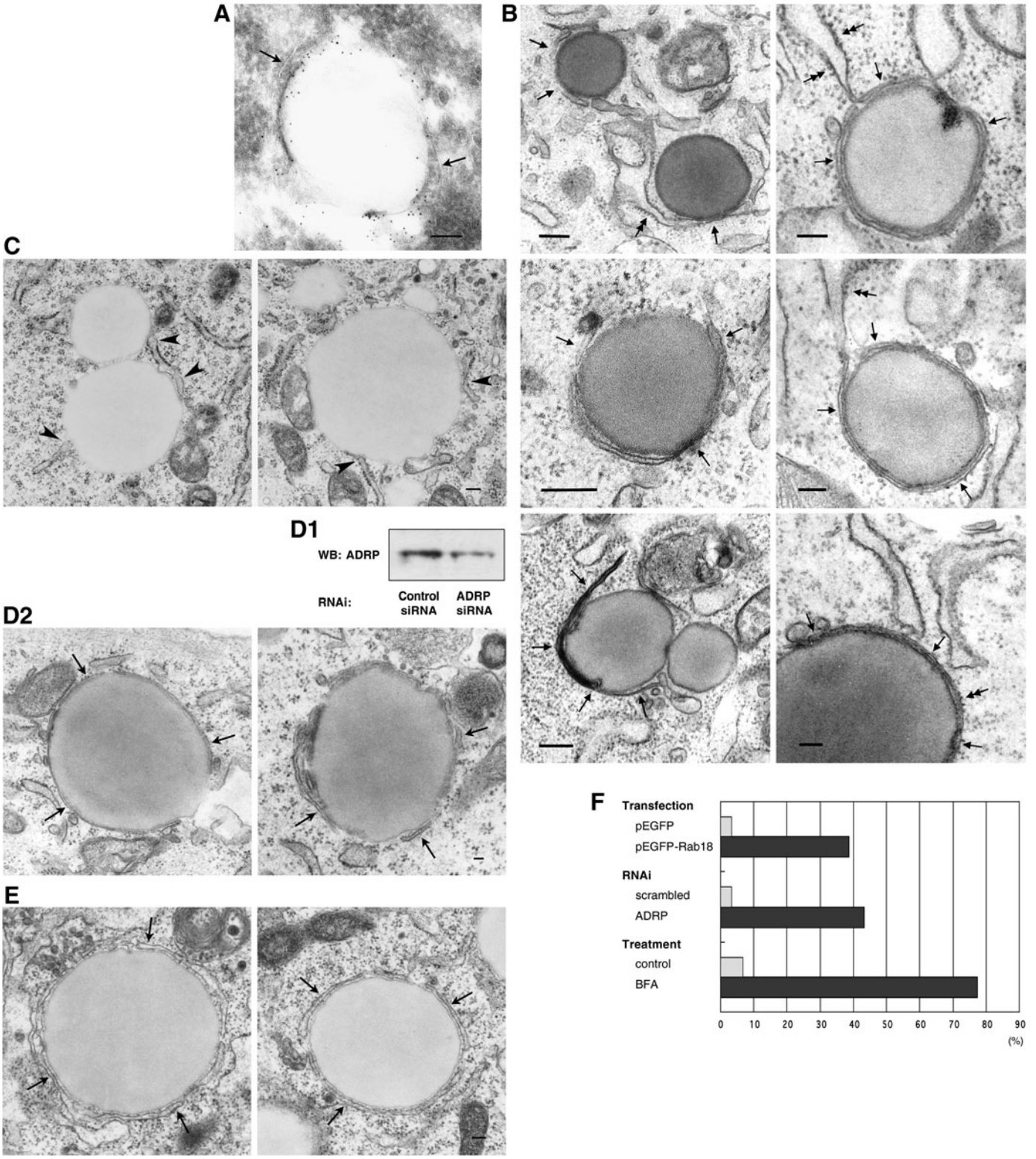

Fig. 5. See next page for legend.

Mechanism by which reduction of ADRP induces LD-ER apposition

We showed that reduction of ADRP in LDs causes close apposition of LDs and the ER-derived membrane. The detailed function of ADRP in LDs has not been determined, but its overexpression was shown to stimulate LD formation (Imamura et al., 2002; Nakamura and Fujimoto, 2003) and its reduction was reported to result in a decrease in LDs detectable by fluorescence labeling (Nakamura et al., 2004). These results suggested that ADRP is important for the maintenance of the LD structure, and that its reduction may compromise the stability of LDs.

Thus, the elimination of ADRP from LDs may be the only function of Rab18, i.e. reduction of ADRP may induce exactly the same results as Rab18 activation. However, it is also possible that Rab18 may activate specific effectors, which then exert downstream functions. For example, Rab18 itself or Rab18 effectors may bind to particular proteins in the ER membrane, and cause the apposition of LDs to a specific sub-compartment of the ER, whereas simple reduction of ADRP may induce nonspecific apposition to bulk ER. This kind of specificity may be important because the LD-ER apposition may be related to lipid transport as discussed in the following section.

Apposition of ER and other organelles

In hepatocytes, LDs are believed to form in an ER sub-compartment enriched with lipid ester-synthesizing enzymes; LDs are likely to be detached from the ER, and then to dock to another ER sub-compartment where lipid esters in the LDs are utilized to generate very low-density lipoproteins (VLDL) (Gibbons et al., 2000; Murphy, 2001) [for a different possible mechanism of LD formation in other cell types, see Robenek et al. (Robenek et al., 2004)]. Thus, LDs and the ER could exist in proximity in two situations: LD formation and LD docking. If the Rab18-induced LD-ER apposition is involved in LD formation, recruitment of Rab18 should be observed concomitantly with lipid esterification. However, upon addition of oleic acid, Rab18 was detectable only at much later times than LDs or ADRP (Fig. 3). This observation suggests that the LD-ER apposition induced by Rab18 may not be related to the LD formation process.

ER has been shown to appose to other organelles (Voelker, 2003; Levine, 2004). The specialized ER region in contact with mitochondria is referred to as the mitochondria-associated membrane, or MAM (Pickett et al., 1980; Rusinol et al., 1994). MAM is enriched with phosphatidylserine synthase (Vance, 1990), and is thought to be involved in transport of phosphatidylserine from the ER to the mitochondria (Voelker, 2003). More recently, close contact with the plasma membrane was reported in yeast, and the apposed ER region is called the plasma membrane-associated membrane, or PAM (Pichler et al., 2001). The apposition between the ER and LDs is observed frequently in various steroidogenic cells, and has been suggested to be involved in mobilization of stored cholesterol esters for steroid synthesis (Rhodin, 1974; Fawcett, 1981). The present result is consistent with this hypothesis. In accordance with the nomenclature of MAM and PAM, we propose that the ER region apposed to LDs should be called the lipid droplet-associated membrane, or LAM.

Although the mechanism of phosphatidylserine transport between MAM and mitochondria is beginning to be elucidated, it is not yet known how the apposition between the ER and other organelles is formed (Voelker, 2003). The present study showed, for the first time, that a Rab protein is involved in apposition of the ER membrane. It would be of interest to determine whether other GTP-binding proteins are also involved in the formation of MAM, PAM and other membrane appositions. A number of questions remain to be answered regarding the apposition: e.g. how stable is it?; how is it regulated?; what kind of proteins and lipids are involved?, etc. Elucidation of the molecular mechanism responsible for the apposition would also lead to an understanding of its function.

Functional heterogeneity of LD

The present results showed that LDs in a cell could have ADRP and Rab18 in variable ratios, which probably reflects the diverse functional states of the LDs. As speculated above, ADRP is likely to stabilize LDs, and its reduction may lead to mobilization of the lipid content. We suppose that Rab18 may offer a physiological mechanism to regulate the amount of ADRP. ARF1 may also be involved in regulation by dissociation of ADRP from LDs (Nakamura et al., 2004). The conjecture that the amount of ADRP is correlated with LD function was supported by the observation that ER-linked LDs lacked ADRP, while independent LDs contained it (Hayashi and Su, 2003).

It is becoming clear that the LD is not a static organelle involved only in storing excessive lipids. The contents of LDs and their relationship to other organelles are regulated by intricate mechanisms, and LDs in different functional states

Fig. 5. (A) Immunogold electron microscopy of HepG2 cells expressing EGFP-Rab18(WT). Ultrathin cryosections were labeled with anti-GFP antibody. Most LDs appeared as vacant round spaces because lipid esters were not retained well in the sections. Gold labeling was observed along the rim of LDs. Notably, thin membrane cisternae were often seen adjacent to the labeled LD (arrows). Scale bar: 100 nm. (B) Conventional electron microscopy of 3T3 cells expressing EGFP-Rab18(WT). LDs were frequently apposed to thin membrane cisternae (arrows). The direct continuity of the membrane cisterna and the rough ER (double arrows in the upper left, upper right and middle right figures), and the ribosomes in the membrane cisterna (double arrows in the lower right figure) were observed in many cases. Scale bars: 100 nm. (C) Conventional electron microscopy of control 3T3 cells. Small ER cisternae were occasionally found adjacent to LDs (arrowheads), but contacts between them were seldom extensive. Scale bar: 100 nm. (D) 3T3 cells treated with siRNA for knockdown of the expression of ADRP. (D-1) Western blotting of ADRP. Cells were treated with control random siRNA or ADRP siRNA, and equal amounts of the total cell lysates (20 μg) were electrophoresed. The expression of ADRP was reduced by more than 50% by this procedure. (D-2) In cells treated with ADRP siRNA, LDs in apposition with thin membrane cisternae were frequently observed (arrows). Scale bar: 100 nm. (E) Conventional electron microscopy of 3T3 cells treated with brefeldin A for 5 hours. Most LDs were surrounded by thin membrane cisternae (arrows). Scale bar: 100 nm. (F) Frequency of 3T3 cells with LDs in close membrane apposition. More than 30 cells were chosen randomly, and only LDs with membrane cisternae apposed to more than half its circumference were counted as positive. The transfection efficiency was no less than 60% as determined by fluorescence microscopy.

must coexist in the cell. The physiological significance of LDs, especially in relation to intracellular lipid homeostasis, should be clarified through further studies of their regulatory mechanisms.

We are grateful to Toshihide Kobayashi (RIKEN), Yasuo Uchiyama (Osaka University), Yoshimi Takai (Osaka University), Toshiaki Katada (Tokyo University), Takuya Sasaki (Tokushima University) and Mitsunori Fukuda (RIKEN) for providing reagents, and to Tetsuo Okumura for technical assistance. This work was supported by Grants-in-Aid for Scientific Research (T.F. and H.T.), the 21st Century COE Program 'Integrrated Molecular Medicine for Neuronal and Neoplastic Disorders' (T.F.), and CLUSTER Project 'Tokushima Proteomics Factory' (H.T.) of the Japanese Ministry of Education, Culture, Sports, Science and Technology.

References

Barbero, P., Buell, E., Zulley, S. and Pfeffer, S. R. (2001). TIP47 is not a component of lipid droplets. *J. Biol. Chem.* **276**, 24348-24351.

Bozza, P. T., Yu, W., Penrose, J. F., Morgan, E. S., Dvorak, A. M. and Weller, P. F. (1997). Eosinophil lipid bodies: specific, inducible intracellular sites for enhanced eicosanoid formation. *J. Exp. Med.* **186**, 909-920.

Brasaemle, D. L., Barber, T., Wolins, N. E., Serrero, G., Blanchette-Mackie, E. J. and Londos, C. (1997). Adipose differentiation-related protein is an ubiquitously expressed lipid storage droplet-associated protein. *J. Lipid Res.* **38**, 2249-2263.

Cole, N. B., Murphy, D. D., Grider, T., Rueter, S., Brasaemle, D. and Nussbaum, R. L. (2002). Lipid droplet binding and oligomerization properties of the Parkinson's disease protein alpha-synuclein. *J. Biol. Chem.* **277**, 6344-6352.

Fawcett, D. W. (1981). *The Cell*. Philadelphia, USA: W. B. Saunders.

Frolov, A., Petrescu, A., Atshaves, B. P., So, P. T., Gratton, E., Serrero, G. and Schroeder, F. (2000). High density lipoprotein-mediated cholesterol uptake and targeting to lipid droplets in intact L-cell fibroblasts. A single- and multiphoton fluorescence approach. *J. Biol. Chem.* **275**, 12769-12780.

Fujimoto, T., Kogo, H., Ishiguro, K., Tauchi, K. and Nomura, R. (2001). Caveolin-2 is targeted to lipid droplets, a new "membrane domain" in the cell. *J. Cell Biol.* **152**, 1079-1085.

Fujimoto, Y., Itabe, H., Sakai, J., Makita, M., Noda, J., Mori, M., Higashi, Y., Kojima, S. and Takano, T. (2004). Identification of major proteins in the lipid droplet-enriched fraction isolated from the human hepatocyte cell line HuH7. *Biochim. Biophys. Acta* **1644**, 47-59.

Fukumoto, S. and Fujimoto, T. (2002). Deformation of lipid droplets in fixed samples. *Histochem. Cell Biol.* **118**, 423-428.

Garcia, A., Sekowski, A., Subramanian, V. and Brasaemle, D. L. (2003). The central domain is required to target and anchor perilipin A to lipid droplets. *J. Biol. Chem.* **278**, 625-635.

Garcia, A., Subramanian, V., Sekowski, A., Bhattacharyya, S., Love, M. W. and Brasaemle, D. L. (2004). The amino and carboxyl termini of perilipin a facilitate the storage of triacylglycerols. *J. Biol. Chem.* **279**, 8409-8416.

Gibbons, G. F., Khurana, R., Odwell, A. and Seelaender, M. C. (1994). Lipid balance in HepG2 cells: active synthesis and impaired mobilization. *J. Lipid Res.* **35**, 1801-1808.

Gocze, P. M. and Freeman, D. A. (1994). Factors underlying the variability of lipid droplet fluorescence in MA-10 Leydig tumor cells. *Cytometry* **17**, 151-158.

Hayashi, T. and Su, T. P. (2003). Sigma-1 receptors (sigma(1) binding sites) form raft-like microdomains and target lipid droplets on the endoplasmic reticulum: roles in endoplasmic reticulum lipid compartmentalization and export. *J. Pharmacol. Exp. Ther.* **306**, 718-725.

Imamura, M., Inoguchi, T., Ikuyama, S., Taniguchi, S., Kobayashi, K., Nakashima, N. and Nawata, H. (2002). ADRP stimulates lipid accumulation and lipid droplet formation in murine fibroblasts. *Am. J. Physiol. Endocrinol. Metab.* **283**, E775-E783.

Kabeya, Y., Mizushima, N., Ueno, T., Yamamoto, A., Kirisako, T., Noda, T., Kominami, E., Ohsumi, Y. and Yoshimori, T. (2000). LC3, a mammalian homologue of yeast Apg8p, is localized in autophagosome membranes after processing. *EMBO J.* **19**, 5720-5728.

Kikuchi, M., Hatano, N., Yokota, S., Shimozawa, N., Imanaka, T. and Taniguchi, H. (2004). Proteomic analysis of rat liver peroxisome: presence of peroxisome-specific isozyme of Lon protease. *J. Biol. Chem.* **279**, 421-428.

Kobayashi, T., Stang, E., Fang, K. S., de Moerloose, P., Parton, R. G. and Gruenberg, J. (1998). A lipid associated with the antiphospholipid syndrome regulates endosome structure and function. *Nature* **392**, 193-197.

Levine, T. (2004). Short-range intracellular trafficking of small molecules across endoplasmic reticulum junctions. *Trends Cell Biol.* **14**, 483-490.

Liou, W., Geuze, H. J. and Slot, J. W. (1996). Improving structural integrity of cryosections for immunogold labeling. *Histochem. Cell Biol.* **106**, 41-58.

Litvak, V., Shaul, Y. D., Shulewitz, M., Amarilio, R., Carmon, S. and Lev, S. (2002). Targeting of Nir2 to lipid droplets is regulated by a specific threonine residue within its PI-transfer domain. *Curr. Biol.* **12**, 1513-1518.

Liu, P., Ying, Y., Zhao, Y., Mundy, D. I., Zhu, M. and Anderson, R. G. (2004). Chinese hamster ovary K2 cell lipid droplets appear to be metabolic organelles involved in membrane traffic. *J. Biol. Chem.* **279**, 3787-3792.

Londos, C., Brasaemle, D. L., Schultz, C. J., Segrest, J. P. and Kimmel, A. R. (1999). Perilipins, ADRP, and other proteins that associate with intracellular neutral lipid droplets in animal cells. *Semin. Cell Dev. Biol.* **10**, 51-58.

Lutcke, A., Parton, R. G., Murphy, C., Olkkonen, V. M., Dupree, P., Valencia, A., Simons, K. and Zerial, M. (1994). Cloning and subcellular localization of novel rab proteins reveals polarized and cell type-specific expression. *J. Cell Sci.* **107**, 3437-3448.

McLauchlan, J. (2000). Properties of the hepatitis C virus core protein: a structural protein that modulates cellular processes. *J. Viral Hepat.* **7**, 2-14.

Miura, S., Gan, J. W., Brzostowski, J., Parisi, M. J., Schultz, C. J., Londos, C., Oliver, B. and Kimmel, A. R. (2002). Functional conservation for lipid storage droplet association among Perilipin, ADRP, and TIP47 (PAT)-related proteins in mammals, Drosophila, and Dictyostelium. *J. Biol. Chem.* **277**, 32253-32257.

Murphy, D. J. (2001). The biogenesis and functions of lipid bodies in animals, plants and microorganisms. *Prog. Lipid Res.* **40**, 325-438.

Murphy, D. J. and Vance, J. (1999). Mechanisms of lipid-body formation. *Trends Biochem. Sci.* **24**, 109-115.

Nakamura, N. and Fujimoto, T. (2003). Adipose differentiation-related protein has two independent domains for targeting to lipid droplets. *Biochem. Biophys. Res. Commun.* **306**, 333-338.

Nakamura, N., Akashi, T., Taneda, T., Kogo, H., Kikuchi, A. and Fujimoto, T. (2004). ADRP Is dissociated from lipid droplets by ARF1-dependent mechanism. *Biochem. Biophys. Res. Commun.* **322**, 957-965.

Ohashi, M., Mizushima, N., Kabeya, Y. and Yoshimori, T. (2003). Localization of mammalian NAD(P)H steroid dehydrogenase-like protein on lipid droplets. *J. Biol. Chem.* **278**, 36819-36829.

Ostermeyer, A. G., Paci, J. M., Zeng, Y., Lublin, D. M., Munro, S. and Brown, D. A. (2001). Accumulation of caveolin in the endoplasmic reticulum redirects the protein to lipid storage droplets. *J. Cell Biol.* **152**, 1071-1078.

Ostermeyer, A. G., Ramcharan, L. T., Zeng, Y., Lublin, D. M. and Brown, D. A. (2004). Role of the hydrophobic domain in targeting caveolin-1 to lipid droplets. *J. Cell Biol.* **164**, 69-78.

Pichler, H., Gaigg, B., Hrastnik, C., Achleitner, G., Kohlwein, S. D., Zellnig, G., Perktold, A. and Daum, G. (2001). A subfraction of the yeast endoplasmic reticulum associates with the plasma membrane and has a high capacity to synthesize lipids. *Eur. J. Biochem.* **268**, 2351-2361.

Pickett, C. B., Montisano, D., Eisner, D. and Cascarano, J. (1980). The physical association between rat liver mitochondria and rough endoplasmic reticulum. I. Isolation, electron microscopic examination and sedimentation equilibrium centrifugation analyses of rough endoplasmic reticulum-mitochondrial complexes. *Exp. Cell Res.* **128**, 343-352.

Pol, A., Luetterforst, R., Lindsay, M., Heino, S., Ikonen, E. and Parton, R. G. (2001). A caveolin dominant negative mutant associates with lipid bodies and induces intracellular cholesterol imbalance. *J. Cell Biol.* **152**, 1057-1070.

Pol, A., Martin, S., Fernandez, M. A., Ferguson, C., Carozzi, A., Luetterforst, R., Enrich, C. and Parton, R. G. (2004). Dynamic and regulated association of caveolin with lipid bodies: modulation of lipid body motility and function by a dominant negative mutant. *Mol. Biol. Cell* **15**, 99-110.

Prattes, S., Horl, G., Hammer, A., Blaschitz, A., Graier, W. F., Sattler, W., Zechner, R. and Steyrer, E. (2000). Intracellular distribution and mobilization of unesterified cholesterol in adipocytes: triglyceride droplets are surrounded by cholesterol-rich ER-like surface layer structures. *J. Cell Sci.* **113**, 2977-2989.

Rhodin, J. A. G. (1974). *Histology, A Text and Atlas*. New York: Oxford University Press.

Robenek, M. J., Severs, N. J., Schlattmann, K., Plenz, G., Zimmer, K. P., Troyer, D. and Robenek, H. (2004). Lipids partition caveolin-1 from ER membranes into lipid droplets: updating the model of lipid droplet biogenesis. *FASEB J.* **18**, 866-868.

Rusinol, A. E., Cui, Z., Chen, M. H. and Vance, J. E. (1994). A unique mitochondria-associated membrane fraction from rat liver has a high capacity for lipid synthesis and contains pre-Golgi secretory proteins including nascent lipoproteins. *J. Biol. Chem.* **269**, 27494-27502.

Tauchi-Sato, K., Ozeki, S., Houjou, T., Taguchi, R. and Fujimoto, T. (2002). The surface of lipid droplets is a phospholipid monolayer with a unique Fatty Acid composition. *J. Biol. Chem.* **277**, 44507-44512.

Umlauf, E., Csaszar, E., Moertelmaier, M., Schuetz, G. J., Parton, R. G. and Prohaska, R. (2004). Association of stomatin with lipid bodies. *J. Biol. Chem.* **279**, 23699-23709.

Vance, J. E. (1990). Phospholipid synthesis in a membrane fraction associated with mitochondria. *J. Biol. Chem.* **265**, 7248-7256.

Voelker, D. R. (2003). New perspectives on the regulation of intermembrane glycerophospholipid traffic. *J. Lipid Res.* **44**, 441-449.

Wolins, N. E., Rubin, B. and Brasaemle, D. L. (2001). TIP47 associates with lipid droplets. *J. Biol. Chem.* **276**, 5101-5108.

Yu, W., Bozza, P. T., Tzizik, D. M., Gray, J. P., Cassara, J., Dvorak, A. M. and Weller, P. F. (1998). Co-compartmentalization of MAP kinases and cytosolic phospholipase A2 at cytoplasmic arachidonate-rich lipid bodies. *Am. J. Pathol.* **152**, 759-769.